International Journal of Mass Spectrometry 507 (2025) 117352

Contents lists available at ScienceDirect

International Journal of Mass Spectrometry

journal homepage: www.elsevier.com/locate/ijms

Gas phase proton affinities of proline-containing peptides. 1: ProGly, ProAla, ProVal, ProLeu, ProIle, and ProPro☆

Henry Cardwell [a], Paul Acoria [b], Alexis Brender A Brandis [a], Kathy Huynh [a], Madeleine Lamb [a], Sophie Messinger [a], Daria Moody [a], Laurel Nicks [a], Hao Qian [a], Marcus Quint [b], Trinh Ton [a], Anna Grace Towler [a], Michael Valasquez [b], Jennifer Poutsma [b,**], John C. Poutsma [a,*]

[a] The Department of Chemistry, The College of William and Mary in Virginia, Williamsburg, VA, 23187-8795, USA
[b] The Department of Chemistry, Old Dominion University, Norfolk, VA, 23529, USA

ARTICLE INFO

Keywords:
Peptide
Proton affinity
Proline effect
Kinetic method
DFT calculations

ABSTRACT

The gas-phase proton affinities (PA) for a series of proline-containing dipeptides have been measured in an ESI triple quadrupole instrument using the extended kinetic method. Proton affinities for ProGly (**1**), ProAla (**2**), ProVal (**3**), ProLeu (**4**), ProIle (**5**), and ProPro (**6**) were determined to be 969.6 ± 7.8, 990.4 ± 7.7, 987.6 ± 7.9, 982.8 ± 8.0, 988.8 ± 10.1, and 996.5 ± 12.2 kJ/mol, respectively. Predictions for the proton affinities for **1**–**6** were also obtained through isodesmic calculations at the B3LYP/6-311++G(d,p)//B3LYP/6-31+G(d) level of theory. The predicted proton affinities for **1** and **6** of 966.9 and 991.0 kJ/mol are in agreement with the experimental values. However, the predicted proton affinities for **2**–**5** of 973.5, 975.9, 975.7, and 975.9 are between 8 and 15 kJ/mol lower than the experimental values. Additional calculations with a larger basis set (B3LYP/6-311++G(2df,2p), inclusion of dispersion (B3LYP-D3/6-311++G(d,p)), switching to second order perturbation theory (MP2/6-31++G(d,p) and MP2/6-311++G(2df,2p), or switching density functional (M06-2x/6-311++G(d,p) and M06-2x/6-311++G(2df,2p) show only modest changes in derived thermochemistry lending support to the original calculations. We recommend using the experimental proton affinities for ProGly and ProPro and using the calculated values for ProAla, ProVal, ProLeu, and ProIle with the experimental proton affinities as upper limits.

1. Introduction

Automated peptide sequencing forms the basis for modern tandem mass spectrometry-based proteomics studies [1–5]. In bottom-up experiments, the protein of interest is digested into peptides by a proteolytic enzyme such as trypsin and the peptides are analyzed by HPLC-tandem mass spectrometry. If low-energy collision-induced dissociation is used to fragment the peptides, backbone amide cleavages occur resulting mainly in b_n + - and y_m + -type ions [6] depending on the residues involved and the overall charge of the peptide [7]. The mobile proton model governs the fragmentation behavior of peptides when the number of added protons exceeds the number of basic residues in the peptide [8–10]. The first step in the mobile proton model involves the transfer of one of the ionizing protons to an amide site upon collisional activation. For ease of automated sequencing, one desires the proton to be non-selectively transferred to multiple different amide sites, resulting in random fragmentation along the peptide backbone. Computer-based algorithms can then match predicted fragmentation spectra for candidate peptides with the experimentally generated product ion spectrum to allow for peptide determination, and ultimately the protein of interest in the proteomics experiment [11–15].

Certain amino acid residues can lead to selective cleavages that suppress random cleavages and confound automated sequencing algorithms [16–32]. One such residue is proline, which tends to cause a selective cleavage N-terminal to the residue known as the “proline effect” [16,17,19,20,24–30]. Proline is the only protein amino acid that has a secondary amine at the N-terminus and has a proton affinity of 941 kJ/mol, which is much larger than other aliphatic amino acids

☆ Dedicated to Professor Richard O'Hair on the occasion of his 60th birthday for many years of continued friendship and scientific inspiration.

* Corresponding author.
** Corresponding author.
E-mail addresses: jlradkie@odu.edu (J. Poutsma), jcpout@wm.edu (J.C. Poutsma).

https://doi.org/10.1016/j.ijms.2024.117352
Received 15 July 2024; Received in revised form 22 September 2024; Accepted 5 October 2024
Available online 24 October 2024

[33–35]. When inserted into peptides, proline forms a tertiary amide, and the enhanced basicity of this amide site was thought to play a role in the proline effect. Vaisar and Urban studied the fragmentation behavior of AVXLG (X = Pro, Pipecolic acid (Pip), the 6-membered ring analog of proline, and N-methylalanine(NME)) and found that for X = Pro, the y_3^+ "proline effect" fragment was the dominant fragmentation product, whereas for X = Pip and NME, fragmentation C-terminal to the X residue to give b_3^+ was dominant [19]. For X = Pro and Pip, the resulting b_3^+ oxazolone ion is bicyclic and the authors postulated that the instability of the bicyclic AVP b_3^+ ion shuts down that channel and results in enhanced production of the y_3^+ "proline effect" fragment. Paizs and co-workers studied the fragmentation of AAXPA (X = A, S, L, V, F) peptides in which all species except AASPA gave a strong y_2^+ "proline effect" fragment. In their computational study, they found that the amide oxygen between A_3 and P_4 in AAAPA is the most basic amide site and they concluded that protonation at this site is favored in the early phase of dissociation [30].

In some of our earlier collaborative work with the Wysocki group, we confirmed that the proline effect is a combination of the enhanced basicity of the proline residue and the conformational rigidity of the constrained five-membered ring [36]. We also discovered a new selective cleavage for the six-membered ring analog, pipecolic acid (Pip), which results in b_n + C-terminal to the Pip residue. Our results have been confirmed by theoretical work by Bythell [37] and by cold-ion spectroscopy experiments by McLuckey and Zwier [38].

A data mining analysis of over 28,000 peptide fragmentation spectra found that certain residues, such as Cys, Pro and Gly, tend to cause a decrease in fragmentation efficiency when N-terminal to proline, whereas others, such as Ile, Leu, and Val, lead to enhanced cleavage when N-terminal to proline [26,29]. The Wysocki group has also shown that the structures of peptide fragments containing proline also depends on the nature of the preceding residue with GP, AP, VP, LP and IP b_2^+ ions predominantly forming oxazolones [39] with only HP b_2^+preferring a diketopiperazine structure. Finally, the structure of proline-containing b_2^+ ions has been shown to also depend on the residue C-terminal to proline, as PP b_2^+ from protonated PPP forms a diketopiperazine structure [40], whereas PP b_2^+ from protonated PPG forms an oxazolone [41]. Clearly, the individual residues near the proline are playing an energetic role in the peptide fragmentation process.

In an effort to better understand the effects that differing residues play in the fragmentation process, we have undertaken a comprehensive study of the structure and acid-base properties of all 39 proline-containing dipeptides and 40 Pip-containing dipeptides using the extended kinetic method and density functional theory calculations. In contrast to the amino acids themselves, there have been relatively few experimental studies of the absolute gas-phase acid/base properties of small peptides. Early ICR-bracketing studies by Amster and co-workers established the gas-phase basicities (GB) for twenty two valine-containing dipeptides including ValPro and ProVal [42]. Cassady and co-workers have measured the gas-phase basicity of numerous small peptides containing Ala and Gly [43], His or Lys [44], GlyPro, ProGly, and ProPro [45], and Ser [46] again using proton-transfer reactions in an ICR. In calibrating their laser-induced acoustic desorption apparatus, Kenttämaa and co-workers investigated the gas-phase basicities of several dipeptides, including AlaAla and ValPro, and found excellent agreement with earlier studies indicating that the LIAD process did not produce excited di-peptides during the desorption process [47]. No attempts were made to vary the temperature of these experiments, so there have been no direct proton affinity measurements for proline-containing peptides. Herein, we present experimental and computational results for the six aliphatic ProXxx dipeptides: ProGly (**1**), ProAla (**2**), ProVal (**3**), ProLeu (**4**), ProIle (**5**), and ProPro(**6**).

2. Experimental and theoretical methods

2.1. Kinetic method experiments

All experiments were performed in a ThermoScientific TSQ Quantum Ultra triple quadrupole instrument equipped with an IonMax ESI source. Full experimental details have been presented elsewhere [33,48]. Dilute solutions (*ca.* 1–10 × 10^{-3} M) of a peptide and one of a series of reference bases in slightly acidified (1 % formic acid) 50:50 methanol:water were directly infused into the electrospray ionization source of the TSQ at flow rates between 5 and 10 μL/min. Electrospray and ion focusing conditions were varied in order to maximize the ion count for the proton-bound heterodimer $[A–H^+–B_i]^+$. The proton-bound dimer ions were isolated in Q1 at a resolution of 0.8–1.0 amu and were allowed to pass into the rf-only collision cell (q2). The isolated ions are allowed to undergo collision-induced dissociation with argon gas maintained at a pressure of 0.5 mTorr. Product ion spectra were recorded at collision energies between 0 and 30 V (lab, equal to the Q2 pole offset voltage). The intensities of each primary product ion and any secondary product ions were recorded and analyzed using standard extended kinetic method (EKM) techniques [49–53]. Secondary product ion intensities were added to the corresponding primary product intensities before undergoing EKM analysis. Experiments were repeated on at least three different days and were averaged to give the final ratios $\ln[B_iH^+/AH^+]$ for use in the EKM workup.

Enthalpy (PA) and entropy contributions (ΔS_{prot}) for **1**–**6** were obtained from the extended kinetic method (EKM) that has been described in detail elsewhere [49–53]. This method requires a plot of $\ln(I_{[BiH+]}/I_{[AH+]})$ vs. $PA_{Bi} - PA_{avg}$, where $I_{[BiH+]}$ and $I_{[AH+]}$ are the intensities of the protonated reference base and peptide products, PA_{Bi} is the proton affinity of the ith reference base, and PA_{avg} is the average proton affinity of the set of *i* reference bases. The Orthogonal Distance Regression (ODR) method as implemented in the ODR-pack program of Ervin and co-workers was used to extract proton affinities and protonation entropies from the data [53]. In this method all ln(intensity ratios) for *m* reference bases at *n* collision energies are analyzed simultaneously. A total of *n* lines are generated and forced to cross at a single isothermal point, which gives the proton affinity and protonation entropy for the peptide under study. This method also gives a realistic estimation of the errors in the derived quantities by using Monte Carlo simulations to determine isothermal points from randomly-perturbed intensity ratios. For these studies, we used a window of ±5 kJ/mol in the reference acidity/basicity values and a window of ±0.05 for the ln(ratio) values. Proton affinity and protonation entropy values are reported with error bars corresponding to ±1 standard deviation, as determined from the Monte Carlo simulations.

2.2. Computational methods

Predictions for the proton affinities of **1**–**6** were also obtained from hybrid density functional theory calculations. All *ab initio* and density functional theory calculations were performed using the Gaussian09 or Gaussian16 suites of programs [54,55]. The GMMX conformer searching routine in PCModel [56] was used to find conformations within 60 kJ/mol of the minimum-energy structure for all neutral and cationic species. These structures are used as starting points for a series of *ab initio* and density functional theory calculations of progressively higher levels of theory. Ultimately, geometries and harmonic vibrational frequencies for neutral **1**–**6**, and various N-protonated forms were calculated at the B3LYP/6-31+G(d) level [57,58]. Zero-point energy (ZPE) and thermal corrections were obtained from un-scaled harmonic vibrational frequencies. Total electronic energies were obtained using single-point energy calculations at the B3LYP/6-311++G(d,p) level and are combined with ZPE, thermal corrections, and a PV work term to give 298 K enthalpy values. Total entropies were taken from the Gaussian09 output without scaling. Gibbs free energies were calculated by adding

the "thermal correction to Gibbs Free Energy" obtained from B3LYP/6-31+G(d) frequency calculations to the B3LYP/6-311++G(d,p) single-point energies.

Predictions for the proton affinities for **1**–**6** were computed directly from calculated enthalpies at 298 K according to reaction 1. For all of the peptides in this study, we were able

$$AAH^+ \rightarrow AA + H^+ \quad (1)$$

to locate multiple low-energy conformers. Thermochemical values presented here are Boltzmann-weighted enthalpy values for the different conformers obtained by determining relative gas-phase populations based on G_{298}. We chose the B3LYP/6-311++G(d,p)//B3LYP/6-31+G(d) level of theory based on previous work on proton affinities of amino acids [33,59–63] in which the B3LYP/6-311++G(d,p)//B3LYP/6-31+G(d) method gave nearly quantitative agreement with experimental PAs for a variety of nitrogenous bases including dimethylamine, isopropylamine, ethylenediamine and glycine [64]. Despite the excellent agreement for absolute proton affinities with literature values, we report here predictions for PA from isodesmic reaction 2, using proline as a reference base with a known proton affinity of 941 kJ/mol [64].

$$PeptideH^+ + Pro \rightarrow Peptide + ProH^+ \quad (2)$$

Additional calculations were performed for conformers within 10–20 kJ/mol of the global minimum structures of **1**–**6** to test for the size of the basis set, electronic structure method, and the inclusion of dispersion. Single point energy calculations were performed at the B3LYP/6-31+G(d) geometries with the following levels: B3LYP/6-31++G(2df,2p), B3LYP-D3/6-311++G(d,p) including Grimme's DFT-D3 dispersion corrections [65], MP2/6-311++G(d,p) [66], and MP2/6-311++G(2df,2p) [66]. Furthermore, the geometries for these selected conformers were re-optimized using the M06-2x/6-31+G(d) functional followed by a single-point energy calculation at the M06-2x/6-311++G(d,p) and M06-2x/6-311++G(2df,2p) levels of theory [67].

3. Materials

ProGly, ProAla, ProVal, ProLeu, ProIle, and ProPro were purchased from Sigma Aldrich or AnaSpec. All reference bases were purchased from Sigma-Aldrich and were used without further purification. All solutions are made with HPLC grade methanol (Sigma-Aldrich) and 18 MΩ H_2O (Millipore).

4. Results and discussion

4.1. Experimental proton affinity measurements

The absolute proton affinity for **1** was obtained using the extended kinetic method as described in the Experimental section. Measured proton affinities for **1**–**6** are shown in Table 1. Fig. 1 shows the first kinetic method plot for **1**, in which five reference bases (3-picoline, pyrrolidine, piperidine, 3,5-lutidine, and 4-tert-butylpyridine) and seven activation energies (6, 9, 12, 15, 18, 21, and 24 V (lab) were used. A list of all reference compounds used in the study and their proton affinities is given in Table 2. Orthogonal distance regression gives an isothermal point of 17.5, 2.5, which corresponds to a derived proton affinity of 969.3 ± 7.8 kJ/mol and a protonation entropy of −20.5 ± 4.8 J mol^{-1} K^{-1}. The uncertainty values were obtained from Monte Carlo simulations with a window of ±5 kJ/mol for the proton affinity and 0.15 for the ln(ratio).

Similar procedures were used to determine experimental proton affinities for **2**–**6**. First kinetic method plots for **2**–**6** are shown in Figures S1 and S4–S7. For **2**, five reference bases and seven collision energies were used, as shown in Figure S1. The ODR-derived isothermal point is 33.6, 4.4, which leads to a derived proton affinity of 988.0 ± 8.1 kJ/mol and a protonation entropy of −36.3 ± 2.0 J mol^{-1} K^{-1}. Five reference bases and seven energies yield the first kinetic method plot for **3** shown in Figure S4. A proton affinity for **3** of 987.0 ± 8.0 and a protonation entropy of −32.6 ± 5.5 J mol^{-1} K^{-1} were derived from ODR analysis. Proton affinities for **4** and **5** of 986.4 ± 8.8 and 986.1 ± 10.1 were obtained from ODR analysis. Protonation entropies for **4** and **5** of −40.1 ± 7.9 and −39.7 ± 8.1 were also obtained. The same five reference bases and seven activation energies were used for **4** and **5** and their first kinetic method plots are shown in Figures S5 and S6. Finally, for **6**, 5 reference bases and seven activation energies were used to derive a proton affinity of 996.5 ± 6.1 and a protonation entropy of −22.3 ± 3.9 J mol^{-1} K^{-1} as shown in Figure S7.

The derived protonation entropy terms are between −20 and −40 J mol^{-1} K^{-1}, which indicates a decrease in entropy upon protonation. This is a result of increased hydrogen bonding in the cations as compared to the neutrals. By comparison, similar kinetic method experiments on proline from our lab resulted in a protonation entropy of −6 J mol^{-1} K^{-1} [33]. These entropic results are consistent with the calculated geometries as discussed below.

Table 1
Experimental and computed 298 K proton affinities for **1**–**6**.

Compound	PA (kJ mol^{-1})	ΔS_p (J mol^{-1} K^{-1})	calc PA (kJ mol^{-1}), raw	calc. PA (kJ mol^{-1}), iso[a]
1	969.3 ± 7.8	−20.5 ± 4.8	966.1	966.9
2	988.0 ± 8.1	−36.3 ± 2.0	972.7	973.5
3	987.0 ± 8.0	−32.6 ± 5.5	975.1	975.9
4	986.4 ± 8.8	−40.1 ± 7.9	974.9	975.7
5	986.1 ± 8.6	−39.7 ± 8.1	975.1	975.9
6	996.5 ± 6.1	−22.3 ± 3.9	990.2	991.0

[a] Isodesmic reference: proline (PA = 941 kJ/mol, ref 35).

4.2. Computational proton affinity predictions

4.2.1. ProGly

Fig. 2 shows the lowest-energy conformers for **1** and $\mathbf{1H}^+$. Figure S8a and b shows the structures and relative energetics for all conformers for **1** and $\mathbf{1H}^+$ within 15 kJ/mol (298 K Gibbs free energy) of the respective global minima, as well as selected additional high-lying conformers with distinct geometric features. The lowest free-energy conformers for **1** all contain a strong hydrogen bond (~2.15 Å) between the nitrogen atom of the proline ring and the hydrogen atom of the NH group in the amide resulting in an "anti" arrangement between the ring nitrogen atom and the amide carbonyl oxygen. Our naming convention for the ProGly and $ProGlyH^+$ conformers is as follows: 1) structures are numbered by relative free energy, and 2) structures are given a description that specifies: *trans(t)* or *cis(c)* peptide bond; the number of the puckered carbon of the proline ring (1-5, see scheme below) and its pucker orientation with respect to the rest of the molecule (endo or exo); the C(=O)-N-C(α)-C(=O) bond dihedral angle; the N-C(α)-C=O dihedral angle; the orientation of the OH group of the COOH moiety (*syn* or *anti*), and finally alternative H-bonding schemes or protonation sites, if necessary. The lowest free energy conformer,

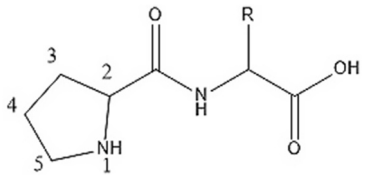

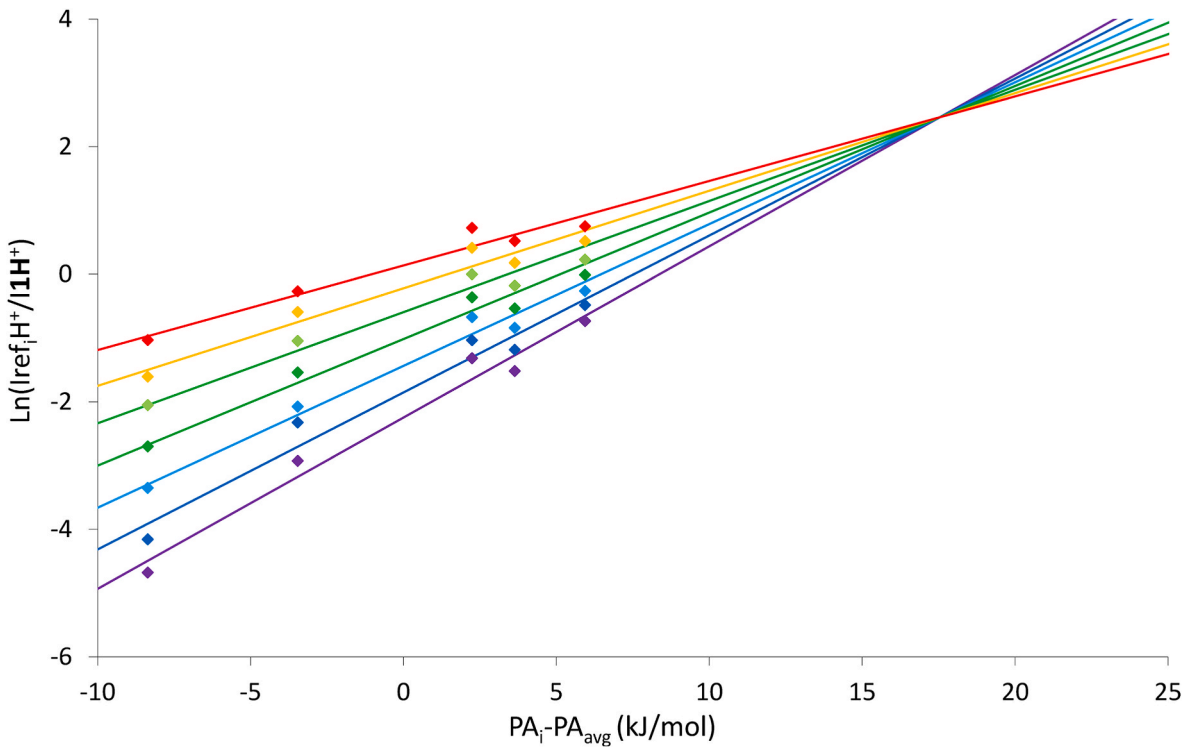

Fig. 1. First kinetic method plot of ln(Ref_iH^+/**1H**$^+$) versus PA-PA_{avg} (kJ/mol). Best-fit lines generated from ODR-derived effective temperatures.

Table 2
Reference bases for kinetic method experiments.

Reference Base	PA	1	2	3	4	5	6
3-picoline	943.4	X	X				
pyrrolidine	948.3	X	X	X			
piperidine	954.0	X	X	X	X	X	
3,5-lutidine	955.4	X					
4-t-butylpyridine	957.7	X		X	X	X	
2,4-lutidine	962.9			X	X	X	
1-methylpyrrolidine	965.6				X	X	X
diisopropylamine	971.9		X	X	X	X	X
di-secbutylamine	980.7						X
triethylamine	981.8						X
2,2,6,6-tetramethylpiperidine	987.0						X

ProGly_001, is therefore t, 4exo, 120, 0, *syn*. The next lowest free energy conformer has the same dihedrals, but the proline ring is puckered in the *endo* orientation (ProGly_002: t, 4endo, 12, 0, *syn*). The 16 lowest-free-energy conformers have the same N-H-N hydrogen-bonding arrangement with differing orientations of the C-terminal portion of the dipeptide. The four lowest free-energy conformers have the carbonyl group of the Gly residue either above or below the plane of the hydrogen bonded nitrogen atoms, while the in-plane arrangement (progly_005:t, 4endo, 180, 0, syn) lies approximately 2.5 kJ/mol higher in free energy (Figure S8a). The additional NH—O=C hydrogen bond (~2.4 Å) afforded by the in-plane arrangement causes this conformer to be the lowest enthalpy conformation for ProGly. Similarly, the second lowest enthalpy conformer contains an *anti*-OH arrangement (progly_008: t, 4endo, 75, 120, anti) and an additional OH—O=C hydrogen bond (1.75 Å). Interestingly, at the B3LYP/6-311++G(d,p) level the 4*exo* arrangement for the proline ring is generally lower in free energy, while the 4*endo* arrangement is preferred with respect to enthalpy.

A differing H-bonding motif in which the hydrogen atom on the NH group of the proline ring is hydrogen bonded to the amide carbonyl oxygen (2.26 Å) was located at a relative free energy of 11.4 kJ/mol (progly_017: t, 4exo, 180, 0, syn, NH-O=C; Figure S8a). The lowest-free-energy conformer with a *cis* peptide bond (progly_054: c, 4exo, NH-O=C, 180, 0, syn) was found to lie 31.0 kJ/mol above progly_001 (Table S1). In total, 110 conformers were located within 60.2 kJ/mol of the global minimum. Complete lists of all located conformers for **1** and **1H**, their calculated 298 K free energies, 298 K enthalpies, and their relative free energies are given in Supporting Information Tables S4 and S5. Similar Tables for **2**–**6** and **2H – 6H** are given in Tables S6–S15 of Supporting Information.

For **1H**$^+$, the lowest-free-energy conformer (proglyh_001, t, 4endo, 180, 0, syn) is protonated on the proline nitrogen atom and has an H-bond between that hydrogen atom and the amide carbonyl oxygen as shown in Fig. 2. As with the neutral, the 14 lowest-free-energy conformers have the same N-H-O hydrogen bonding motif with differing orientations of the glycine end of the dipeptide (Figure S8b). The hydrogen bond length drops considerably to near 1.8 Å indicating a strengthening of the hydrogen bonding network upon protonation, consistent with the large negative entropy change upon protonation. In contrast with the neutral, the lowest-free energy conformer and the lowest enthalpy conformer are the same and involve an additional hydrogen bonding interaction between the Gly carbonyl oxygen atom and the backbone NH (2.15 Å). Higher energy conformers involve rotation about the N-C and C-C single bonds of the Gly residue (Figure S8b). The lowest-energy conformer for **1H**$^+$ with a *cis*-peptide bond lies 17.5 kJ above the global minimum conformer. In total, 48 ring-protonated conformers were located within 74.2 kJ/mol of the minimum energy structure, far fewer than for progly as a result of the stronger hydrogen-bonding network in the cation.

We also investigated the energetics of protonation at the amide carbonyl oxygen and nitrogen atoms. The lowest free-energy CO-protonated species (proglyh_042) lies at a relative energy of 56.1 kJ/mol, whereas the lowest free-energy amide N-protonated protomer (progly_056) lies 102.8 kJ/mol above proglyh_001. An additional 6 amideO conformers and 38 amideN conformers were located. Using the 298 K Gibbs free energy as the weighting factor, 298 K Boltzmann-weighted enthalpy values were obtained for **1** and **1H**$^+$ and lead to a proton

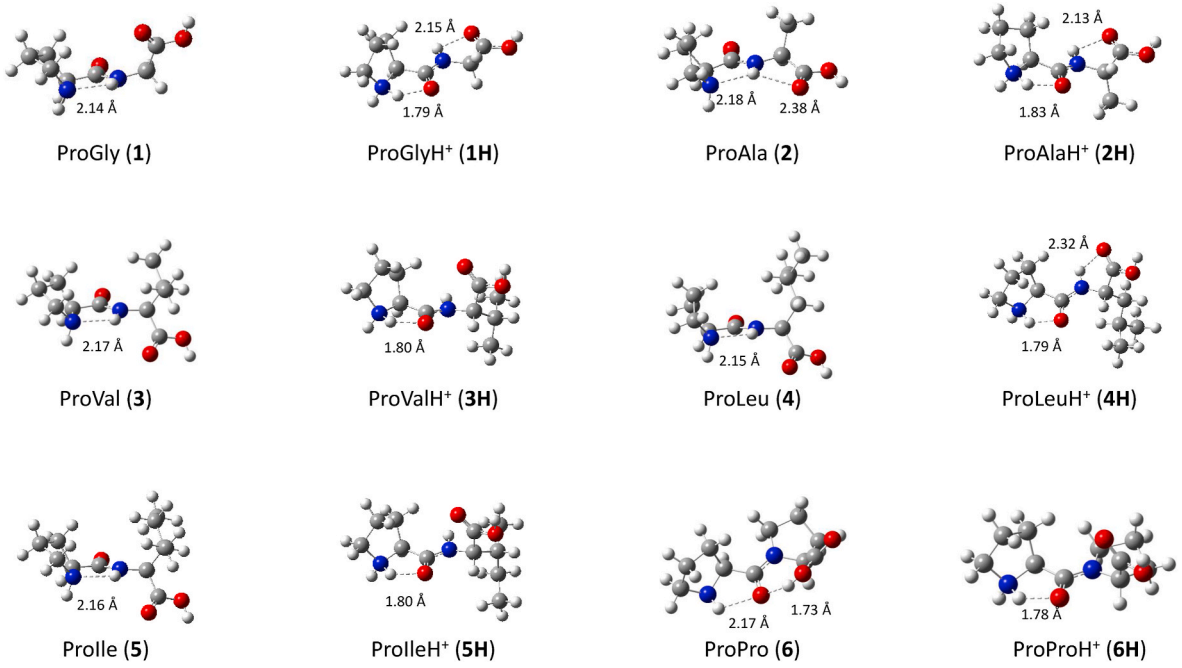

Fig. 2. Lowest energy structures for **1**–**6** and **1H**–**6H** at the B3LYP/6-311++G(d,p)//B3LYP/6-31+G(d,) level of theory.

affinity of 966.1 kJ/mol, in excellent agreement with the experimental value of 969.3 ± 7.8 kJ/mol.

In our previous work on amino acids, the B3LYP/6-311++G(d,p)//B3LYP/6-31+G(d) method provided predictions for proton affinities that were in excellent agreement with our experimental kinetic method affinities [33,59–63]. Nevertheless, we have always reported isodesmic proton affinities with various amines or amino acids serving as the reference compound in order to try to mitigate systematic deficiencies in the chosen computational method. In this study, it makes sense to use proline as the isodesmic reference as its thermochemistry has been well established by Bouchoux and co-workers. Using the kinetic method and high-level calculations, they recommend a 298 K proton affinity of 941.0 kJ/mol for proline [35]. We used a similar procedure for calculating the PA for proline at the B3LYP/6-311++G(d,p) level and a Boltzmann-weighted PA of 940.2 kJ/mol was obtained. Using proline as the isodesmic reference, a prediction for the 298 K PA for ProGly of 966.9 kJ/mol is derived, also in excellent agreement with the experimental proton affinity. Calculated raw and isodesmic proton affinities for **1**–**6** are given in Table 1. Estimates for the proton affinity of **1** at the amide carbonyl oxygen and nitrogen atoms of 910.7 and 862.3 kJ/mol are obtained by adding the difference in enthalpy between the lowest enthalpy amide O/N-protomer and the lowest enthalpy ring protomer to the isodesmic proton affinity (Tables S2 and S3).

The B3LYP/6-311++G(d,p)//B3LYP/6-31+G(d) method that we use for calculating proton affinities is by today's standards rather modest in size. We chose to continue using it for this study of proline-containing dipeptides for two reasons. First, it allows for comparison with previous thermochemical studies from our lab using the same method. Second, for dipeptides with larger side chains (Arg, Lys, His, Trp, Tyr, Phe, etc.) it may not be possible to use larger basis sets or more computationally-intensive methods on our in-house servers. The relatively small dipeptides described in this manuscript are small enough to test the efficacy of our method by changing basis sets and model chemistries and seeing the effects on the derived proton affinities. For ProGly, we investigated the 15 lowest-free-energy conformers (within 8.8 kJ/mol of the global minimum) for the neutral and the 8-lowest-energy conformers (within 17.5 kJ/mol) for the cation at several different levels of theory. A summary of the Boltzmann-weighted proton affinities at different levels of theory for ProGly is given in Table 3 and the relative energies for the various conformers are given in Figure S8a and b.

Increasing the basis set of the single-point energy calculation to B3LYP/6-311++G(2df,2p) results in only slight deviations in the relative free-energy of the conformers for **1** and **1H** with the (progly_001: t, 4exo, 120, 0, syn) and (proglyh_001: t, 4endo, 180, 0, syn) conformers remaining lowest in free energy for the neutral and N-protonated species. Similar calculations for Pro and ProH $^+$ lead to a derived isodesmic proton affinity for **1** of 967.3 kJ/mol; a change of only 0.4 kJ/mol. Including dispersion at the B3LYP-D3/6-311++G(d,p)/6-31+G(d) level results in a somewhat larger increase in the derived isodesmic proton affinity of 1.2 kJ/mol giving 968.1 kJ/mol. The addition of dispersion also reverses the relative ordering of the 4endo and 4exo conformers of neutral **1** with the (progly_002: t, 4endo, 120, 0, syn) arrangement lying 1.0 kJ/mol lower in energy; the lowest energy cation remains the same. Single-point energy calculations using the second order perturbation theory method MP2/6-311++G(d,p) leads to only a slight change in proton affinity of 0.5 kJ/mol, whereas a larger increase of 1.8 kJ/mol was found for single-point energy calculations at the MP2/6-311++(2df,2p) level. Both MP2 levels also predict that the (progly_002: t, 4endo, 120, 0, syn) conformation for **1** lies lowest in energy. For **1H**, MP2/6-311++G(d,p) predicts that the (progyh_003: t, 4endo, −75, 0, syn) conformer without the additional NH—O=C hydrogen bond is the global free energy minimum, whereas MP2 with the larger basis set indicates that the (proglyh_001: t, 4endo, 190, 0, syn) conformer with the additional hydrogen bond lies lowest.

We re-optimized the geometries of the selected conformers using the M06-2x/6-31+G(d,) method followed by single-point energy calculations at the M06-2x/6-311++G(d,p) and M06-2x/6-311++G(2df,2p) levels to gauge the sensitivity of the derived values on the specific density functional theory optimization method. During the re-optimizations, all the ProGly conformers remained in the same orientation during the optimization process, but the relative ordering of the conformers changed slightly. For these levels of theory, the (progly_004: t, 4endo, −120, 0, syn) conformer for **1**, which has a different orientation of the Gly end of the dipeptide, has the lowest free energy. For the cation the (proglyh_003: t, 4endo, −75, 0, syn) conformer without the additional NH—O=C hydrogen bond is the global minimum at the 6-31++G(d,p) level while the bigger basis set predicts that proglyh_001 and progly_003 are essentially isoenergetic. As seen in Table 3, a

Table 3
Isodesmic ProXxx proton affinities (kJ/mol) at different levels of theory.

Method	Raw PA ProGly	Raw PA Pro	Iso PA ProGly[a]
B3LYP/6-311++G(d,p)[b]	966.1	940.2	966.9
B3LYP-D3/6-311++G(d,p)[b]	969.8	943.4	967.4
B3LYP/6-311++G(2df,2p)[b]	969.1	942.8	967.3
MP2/6-311++G(d,p)[b]	963.7	937.3	967.4
MP2/6-311++G(2df,2p)[b]	960.6	932.9	968.7
M06-2x/6-311++G(d,p)[c]	955.5	931.5	965.0
M06-2x/6-311++G(2df,2p)[c]	959.9	933.5	967.2
Method	Raw PA ProAla	Raw PA Pro	Iso PA ProAla[a]
B3LYP/6-311++G(d,p)[b]	972.7	940.2	973.5
B3LYP-D3/6-311++G(d,p)[b]	975.1	943.4	972.7
B3LYP/6-311++G(2df,2p)[b]	974.1	942.8	972.3
MP2/6-311++G(d,p)[b]	972.2	937.3	975.9
MP2/6-311++G(2df,2p)[b]	965.1	932.9	973.2
M06-2x/6-311++G(d,p)[c]	963.6	931.5	973.1
M06-2x/6-311++G(2df,2p)[c]	964.0	933.5	971.5
Method	Raw PA ProVal	Raw PA Pro	Iso PA ProVal[a]
B3LYP/6-311++G(d,p)[b]	975.1	940.2	975.9
B3LYP-D3/6-311++G(d,p)[b]	977.7	943.4	975.3
B3LYP/6-311++G(2df,2p)[b]	977.1	942.8	975.3
MP2/6-311++G(d,p)[b]	972.1	937.3	975.8
MP2/6-311++G(2df,2p)[b]	968.0	932.9	976.1
M06-2x/6-311++G(d,p)[c]	964.0	931.5	973.5
M06-2x/6-311++G(2df,2p)[c]	966.0	933.5	973.5
Method	Raw PA ProLeu	Raw PA Pro	Iso PA ProLeu[a]
B3LYP/6-311++G(d,p)[b]	974.9	940.2	975.7
B3LYP-D3/6-311++G(d,p)[b]	977.7	943.4	975.3
B3LYP/6-311++G(2df,2p)[b]	976.7	942.8	974.9
MP2/6-311++G(d,p)[b]	972.1	937.3	975.8
MP2/6-311++G(2df,2p)[b]	968.1	932.9	976.2
M06-2x/6-311++G(d,p)[c]	963.8	931.5	973.3
M06-2x/6-311++G(2df,2p)[c]	964.6	933.5	972.1
Method	Raw PA ProIle	Raw PA Pro	Iso PA ProIle[a]
B3LYP/6-311++G(d,p)[b]	975.1	940.2	975.9
B3LYP-D3/6-311++G(d,p)[b]	977.9	943.4	975.6
B3LYP/6-311++G(2df,2p)[b]	977.5	942.8	975.7
MP2/6-311++G(d,p)[b]	971.7	937.3	975.4
MP2/6-311++G(2df,2p)[b]	968.0	932.9	976.1
M06-2x/6-311++G(d,p)[c]	967.0	931.5	976.5
M06-2x/6-311++G(2df,2p)[c]	968.6	933.5	976.1
Method	Raw PA ProPro	Raw PA Pro	Iso PA ProPro[a]
B3LYP/6-311++G(d,p)[b]	990.2	940.2	991.0
B3LYP-D3/6-311++G(d,p)[b]	993.0	943.4	990.6
B3LYP/6-311++G(2df,2p)[b]	989.2	942.8	987.4
MP2/6-311++G(d,p)[b]	993.6	937.3	997.3
MP2/6-311++G(2df,2p)[b]	985.5	932.9	993.6
M06-2x/6-311++G(d,p)[c]	982.7	931.5	992.2
M06-2x/6-311++G(2df,2p)[c]	981.2	933.5	988.7

decrease of 1.9 kJ/mol in the derived proton affinity for **1** was found for the 6-311++G(d,p) basis set and an increase of 0.3 kJ/mol was found for the 6-311++G(2df,2p) basis set.

Despite the minor changes in the relative free energies of the different neutral and cationic conformers, the Boltzmann-weighted isodesmic proton affinities for **1** at the various different levels of theory are all within 3.7 kJ/mol of each other and are in excellent agreement with our experimental value. We found similar results for **2**–**6**, as described below, which gives us confidence in the B3LYP/6-31+G(d,) level for geometry optimizations and B3LYP/6-311++G(d,p) for single-point energies moving forward with the larger dipeptides.

4.2.2. ProAla

The lowest free-energy structure for **2** has the same N-H-N hydrogen bonding scheme as **1** with the addition of a second hydrogen bond (2.38 Å) between the backbone amide hydrogen atom and the C-terminal carbonyl (proala_001: t, 4endo, −150, 0, syn; Fig. 2), as seen in progly_005, the lowest enthalpic structure for **1**. The lowest enthalpy conformer for **2** lies 2.9 kJ/mol higher in free energy and contains an *anti*-OH group that forms a strong H-bond (1.74 Å) with the amide carbonyl oxygen (proala_004: t, 4endo, −75, −120, anti; Figure S9a) similar to progly_008. The ten lowest free-energy structures all have the same N-H-N hydrogen bonding with varying orientations and hydrogen bonding interactions of the alanine end of the dipeptide. The lowest free-energy *cis*-isomer (proala_035) lies at a relative energy of 27.5 kJ/mol. In all, 72 different conformers were located within 71.4 kJ/mol of the global minimum structure. For **2H,** the lowest free-energy structure is similar to that for **1H** and contains strong hydrogen bonds between the hydrogen on the protonated ring nitrogen and the amide oxygen atom (1.83 Å) as well as between the hydrogen on the amide nitrogen with the C-terminal carbonyl oxygen (2.13 Å) (proala_001: t, 4, exo, −150, 0, syn; Fig. 2). Three additional conformers were located within 10 kJ/mol of the minimum with different ring pucker and/or C-terminal carbonyl hydrogen bonding scheme (Figure S9b). The difference in free energy between the lowest energy *cis*- and *trans*-isomers drops to 17.5 kJ/mol in the cation. In all, 93 N-protonated and amide protonated conformers were located in our conformational search. Isodesmic Boltzmann-weighted proton affinities for the ring nitrogen, amide oxygen, and amide nitrogen of 972.7, 932.5, and 873.9 were obtained at the B3LYP/6-311++G(d,p)/B3LYP/6-31+G(d) level.

In contrast with our results for **1**, the isodesmic proton affinity for **2** of 973.5 kJ/mol is not in agreement with the experimental result of 988.0 ± 8.1 kJ/mol. The difference of nearly 15 kJ/mol is the largest variation between experimental and B3LYP/6-311++G(d,p)-derived proton affinities that we have ever measured in our lab. It was, in fact, this large difference that led us to investigate different computational methods to ascertain whether the B3LYP/6-311++G(d,p)//B3LYP/6-31+G(d) method that worked so well for simple amino acids was somehow unsuited for dipeptides.

We subjected 12 conformers for **2** located within 10 kJ/mol of the global minimum structure to further calculations and the relative energetics are shown in Figure S9a. The B3LYP and MP2-based methods find the (proala_001: t, 4endo, −150, 0, syn) conformer to be the global minimum structure whereas the M06-2x-based methods predicts that the 4endo conformer (proala_002) is lowest in energy. As with **1**, reordering of the relative energy of some of the higher-energy conformers was observed. For **2H**, four conformers are within 10 kJ/mol of the global minimum. These four conformers, the lowest free energy *cis*-isomer, and the lowest energy amide N and O protomers were subjected to further calculations. The B3LYP/6-311++G(2df2p) single point energy calculations are in accord with the B3LYP/6-311++G(d,p) calculations that the (proalah_001: t, 4exo, −150, 0, syn) isomer is the global minimum. The other methods (MP2, M06-2x, and B3LYP-D3) predict that the (proalah_003: t, endo, −75, 0, syn) conformer lies lowest in free energy. This conformer does not have the second H-bond between the amide NH and the C-terminal C=O.

Table 3 shows that the predicted isodesmic Boltzmann-weighted proton affinities for **2** at the different levels are all within 4.3 kJ/mol of each other and with the exception of the MP2/6-311++G(d,p) prediction, the values are within 2.0 kJ/mol of each other. None of the methods indicate a proton affinity greater than 976 kJ/mol and given the similarity in hydrogen bonding schemes between all six neutrals and cations (see below) it seems unlikely that we are missing a low-energy conformation for the cation that is > 10 kJ/mol stable than the ones that we located in our conformational search. This indicates to us that the difference between computational and experimental proton affinity lies in the experimental value. The first kinetic method plots for **1** and **2** in Fig. 1 and Figure S1 do not indicate any anomalous behavior in the experiments; in fact, the fit to the data looks better for **2** than for **1**. The biggest difference is the location of the crossing point, which has a larger *x* and *y* values for **2** (33.6, 4.4) than for **1** (17.5, 2.5). This indicates that entropy is playing a far bigger role in the dissociation of the proton-bound dimer ions for **2** than for **1**. Ideally, one would wish to have

data for references with proton affinities both above and below the isothermal point so that one interpolates rather than extrapolates the crossing point. Unfortunately, for multifunctional bases such amino acids and peptides, entropy effects cause the effective basicity (which drives the ratios) to be far lower than the proton affinity and results in a crossing point above the data set on the *x*-axis. We tried to use reference bases with larger proton affinities to get data closer to the crossing point but were unable to form sufficient cluster ion counts to get statistically meaningful results and are therefore forced to extrapolate the crossing point for all of the dipeptides.

We have used the ODR method for determining final experimental proton affinities and protonation entropies mainly because it gives a realistic estimation of the error in the derived values from Monte Carlo simulations [53]. The original version of the extended kinetic method uses an alternative method of making a second kinetic method plot of the negative intercepts of the lines in plot 1 vs. their slopes [50–53]. Second kinetic method plots for **1** and **2** are shown in Figures S2 and S3. Both plots are highly correlated and the resulting proton affinities for **1** and **2** are 968.3 and 986.3 kJ/mol. ODR, thus changes the resulting values by less than ~2 kJ/mol, so the discrepancy is not likely to be an artifact from the ODR-fitting procedure. We will further discuss the disagreement between the measured and calculated proton affinities for **2** after first describing the computed results for **3**–**6**.

4.2.3. ProVal

The lowest energy structure for ProVal is in accord with the lowest energy conformers for ProGly and ProAla with a strong hydrogen bond (2.17 Å) between the hydrogen on the amide nitrogen and both the nitrogen atom of the ring and the C-terminal carbonyl oxygen as shown in Fig. 2 (progly_003 and proala_007). For **3**, an additional dihedral angle is necessary for determining the relative orientation of the isopropyl side chain. For naming of **3** and **3H**, the N-C(α)-C(β)-H(β) dihedral angle is appended to the end of the conformer name. The lowest free energy structure for **3** is therefore (proval_001: t, 4exo, −120, 0, syn, 180). The added complexity of the side chain leads to an abundance of low-energy conformers, and we located 54 unique conformations within 20 kJ/mol and 231 conformations in total within 61.6 kJ/mol of the global minimum structure. Figure S10a shows the structures and relative energetics of the 20 conformers that lie within 10 kJ/mol of the global minimum structure as well as additional conformations with unique structural features. All of the lowest 20 conformers have the same N-H-N hydrogen bonding scheme, with differing orientations of the valine end of the peptide and/or differing hydrogen bonding interactions of the C-terminal COOH group. The lowest energy conformer with an N-H-O=C H-bonding arrangement and the lowest energy *cis-isomer* lie 10.9 kJ/mol and 29.9 kJ/mol higher in free energy. For **3H**, the lowest ten conformers lie within 7.8 kJ/mol of the minimum-energy structure and all have the same N-H-O=C H-bonding scheme (1.8 Å in provalh_001). The lowest energy *cis*-isomer is 16.5 kJ/mol higher in free energy. Isomers protonated on the amide O and amide N atoms were located 35.5 and 93.8 kJ/mol above provalh_001.

All conformers for **3** and **3H** lying within 10 kJ/mol of the respective lowest energy structures and the lowest energy amideO and amideN protomers were subjected to further computations. For neutral **3**, all of the additional methods except M062x-/6-311++G(2df,2p) found the (proval_001: t, 4exo, −120, 0, syn, 180) isomer to be the global minimum, with the 4endo isomer (proval_002) lying within 1.3 kJ/mol. The endo-configuration is the global minimum at the M06-2x/6-311++G (2df,2p) level. Some differences in relative order were observed between the different methods, especially with the M06-2x-based methods, which tend to find that conformers with multiple H-bonds are preferred even with respect to free energy. For **3H**, the (t, 4endo, −90, 0, syn, 180) isomer is the lowest energy conformer at each of the levels studied. Despite the differences in relative ordering, the Boltzmann-weighted isodesmic PAs for **3** derived from the different methods are all within 2.5 kJ/mol of each other. As with ProAla, the derived isodesmic proton affinity for **3** of 975.9 kJ/mol is lower than the experimental value of 987.6 ± 7.9 kJ/mol.

4.2.4. ProLeu

The side chain of **4** requires two additional dihedral angles to uniquely specify the different conformers: the N-C(α)-C(β)-C(γ) and C (α)-C(β)-C(γ)-H dihedrals, which are appended to the description after the syn/anti designation. Similar to **2** and **3**, the lowest energy conformer for **4** (proleu_001: t, 4endo, −120, 0, syn, −60, 60) has a N-H-N hydrogen bond (2.15 Å) with the side-chain above the plane of the backbone (Fig. 2). The twenty lowest energy conformations all have this same H-bonding arrangement and lie within 9 kJ/mol of proleu_001. The lowest energy conformer with a N-H-O=C H-bonding arrangement, proleu_021, lies 9.5 kJ/mol higher in free energy. The lowest *cis*-isomer lies at a relative energy of 31.9 kJ/mol. The complexity of the side chain allows for a vast number of conformations, and we located 25 conformations within 10 kJ/mol (Figure S11a), 80 within 20 kJ/mol, and 200 within 53.5 kJ/mol of the global minimum. For **4H**, the lowest energy structure (proleuh_001, t, 4endo, −120, 0, syn, 60, 60) is similar to those for **1H-3H** with ring protonation, a N-H-C=O hydrogen bond (1.79 Å), and a second H-bond between the amide NH and the carbonyl oxygen of the C-terminus (2.32 Å). Again, multiple low-lying conformations were located with 13 within 10 kJ/mol and 38 within 20 kJ/mol of proleuh_001. The lowest energy *cis*-isomer, amideO protomer, and amideN protomer are 17.2, 35.4, and 92.1 kJ/mol higher in energy than proleuh_001. In total, 605 unique ring-protonated, amide O protonated, and amide N protonated conformers were located in our search.

The 20 lowest energy conformers for **4**, 14 lowest energy conformers for **4H** (Figure S11b), and the lowest energy amideO and amideN protomers for **4H** were subjected to further calculations. All levels of theory predict that proleu_001 is the lowest energy neutral conformer and the B3LYP and MP2 based methods generally agree in the relative energetics for the higher-lying conformers. M06-2x geometry optimization and 6-311++G(d,p) single point energy calculations give orderings for the higher-lying conformers that are quite different (Figure S11a), again generally favoring multiple internal hydrogen bonds. For **4H**, the agreement for the energetics of the low-energy conformers between the different methods is better. The B3LYP and MP2-based methods agree that the proleuh_001 conformer is the global minimum, while the M06-2x-based levels find that a conformer with the leucine end of the dipeptide rotated 60° (proleuh_002: t, 4endo, −60, 0, syn, −60, 60) lies lowest. The ordering of the higher-lying conformers changes only slightly between methods. As shown in Table 3, the Boltzmann-weighted isodesmic proton affinities for **4** are in excellent agreement, with all values within 4.1 kJ/mol of the B3LYP/6-311++G(d,p) value and ~10 kJ/mol lower than the experimental value of 986.4 ± 8.8 kJ/mol.

4.2.5. ProIle

For **5**, the N-C(α)-C(β)-H and C(α)-C(β)-C(γ)-C(δ) dihedral is added to the name to account for differing orientations of the side chain. The lowest energy conformer (proile_001: t, 4exo, −120, 0, syn, 180, −60) has a similar hydrogen bonding arrangement to **2**–**4** (2.16 Å), with the sidechain above the H-N-H plane. Two nearly isoenergetic conformers: proile_003: t, 4endo, −120, 0, syn 180, 60, which differs only in the orientation of the ring pucker, and proile_002: t, 4endo, −120, 0, syn, 180, 180, which differs in the orientation of the ring pucker and the rotation of the ethyl portion of the side chain were found to lie within 1 kJ/mol of proile_001. We located 25 conformers within 10 kJ/mol of the global minimum structure (Figure S12a), all of which have the same H-bonding arrangement with different arrangements of the side chain. An isomer with NH-O=C H-bonding arrangement was located with a relative free energy of 10.7 kJ/mol. The lowest energy *cis*-isomer is 30.9 kJ/mol higher in free energy than proile_001. In all, 363 unique conformers were located within 70 kJ/mol of the global minimum.

The lowest energy structure for **5H** (proileh001: t, 4endo, −75, -, syn, 180, −60) is similar to the lowest energy structures for **3H** and **4H** with a

N-H-O=C H-bonding arrangement (1.80 Å) and the C-terminal carbonyl group located above the H-bonding plane. The lowest energy *cis*-isomer is only 16.9 kJ/mol higher in free energy. AmideO and amideN protomers were located 31.2 and 90.0 kJ/mol above the lowest free energy ring-protomer.

Twenty-six neutral **5** conformers and nineteen **5H** conformers were subjected to further calculations. The three nearly isoenergetic neutral conformers proile_001-003 remain within 1.4 kJ/mol of each other at the B3LYP-D3/6-311++G(d,p), B3LYP/6-311++G(2df, 2p) and both MP2-based levels, proile_002 is the lowest energy conformer at the B3LYP-D3 level and proile_003 is the lowest energy conformer for the other three levels (Figure S12a). Re-optimization with the M06-2x functional finds that proile_001 is the lowest energy conformer and the other two isomers are slightly less stable at ~3 and ~2 kJ/mol relative free energy with the two different basis sets. For the cation, all of the methods agree that proileh_001 is the lowest energy conformer again with slight differences in the relative ordering of the higher-energy conformers. As shown in Table 3, the agreement in Boltzmann weighted PA for the different methods is excellent with all of the derived PAs within 0.7 kJ/mol of each other. Again, the calculated proton affinity of 975.9 is on the order of 10 kJ/mol lower than the experimental values of 986.1 ± 8.6 kJ/mol.

4.2.6. ProPro

The additional ring of ProPro alters the naming scheme to include the puckering arrangement for the second proline ring. The lowest energy structure (propro_001: t, 5exo, 4endo, −90, −120, anti, NH-O=C) is shown in Fig. 1. As there is no amide hydrogen atom, the dominant hydrogen bonding scheme switches to a hydrogen bond (2.17 Å) between the hydrogen atom on the ring nitrogen atom and the amide carbonyl oxygen atom (NH-O=C) similar to that found in the cations **1H – 5H**. The amide carbonyl oxygen is oriented in a "syn" arrangement to the ring nitrogen atom (N-C(α)-C-O dihedral near 180°), which is different from neutral **1**–**5,** in which this dihedral angle is near 0°. The four lowest energy conformers have a second hydrogen bond between the terminal OH group and the amide carbonyl oxygen atom (1.73 Å in propro_001). Some higher lying configurations have the "anti" arrangement of the ring nitrogen atom and the amide carbonyl oxygen, while maintaining the hydrogen bond between the terminal OH and the amide carbonyl. The lowest energy *cis*-isomer lies only 6.8 kJ (Table S1) higher in energy and this difference drops to below 3 kJ/mol for some of the other levels of theory. Our conformational search identified 72 unique conformers within 39 kJ/mol of propro_001 that differ mainly in the puckering schemes of the two rings. We performed additional calculations on the 20 lowest energy conformers that lie within 10 kJ/mol of the global minimum structure.

The two lowest energy conformers propro_001 and propro_002 were found to be within 1.2 kJ/mol of each other at all of the additional levels except mp2/6-311++G(d,p). These two conformers differ only in the puckering of the N-terminal proline ring. Unlike **1**–**5**, in which geometry re-optimization with M06-2x/6-31+G(d) always gave the same conformer, for **6**, two of the B3LYP/6-31+G(d) minima changed geometries during re-optimization. Propro_003 (Figure S13a) re-optimized to propro_006 and propro_004 reoptimized to a structure that is not a minimum at B3LYP/6-31+G(d) (propro_004b). Both of these rearrangements involve only a change in the puckering arrangement of the N-terminal proline ring.

The lowest energy conformer for **6H** is similar to those for **1H-5H** with a strong hydrogen bond (1.78 Å) between the ring protonated nitrogen atom and the amide carbonyl oxygen. The seven lowest energy conformers have the same H-bonding arrangement with differing ring puckering schemes. The lowest energy *cis*-isomer lies 4.7 kJ/mol above proproh_001. Protomers protonated on the amide carbonyl oxygen and nitrogen atoms were located at relative energies of 67.6 and 93.6 kJ/mol. The nine lowest energy ring N-protonated conformers and the lowest energy O- and N-amide protonated conformers were subjected to further computations. All methods agree that proproh_001 is the lowest energy conformer. Proproh_006 converted to proproh_009 upon M06-2x re-optimization, but the other conformers remained in the B3LYP minima. B3LYP/6-311++G(d,p)//B3LYP/6-31+G(d) gives a Boltzmann-weighted isodesmic proton affinity of 991.0 kJ/mol, which is lower than the experimental value of 996.5 ± 6.0, but is in better agreement than **2**–**5**. The other methods give predictions ranging from 987.4 to 997.3 kJ/mol, which is a somewhat larger spread than for **1**–**5**.

4.3. Agreement between theory and experiment

It is unclear to us why the experimental proton affinities for **2**–**5** are uniformly higher than those predicted by theory. In early studies of the use of the kinetic method for use with multifunctional bases, several groups found that when the kinetic method fails, it tends to underestimate proton affinities for such species [68–70]. This is mainly due to the underestimation of entropy effects, especially in high-energy collisions in which the activated proton-bound dimer ion dissociates before it can completely sample the full potential energy surface [71]. As seen in Tables 1 and 3 and as discussed below, the calculated proton affinities for **2**–**5** from the different computational methods agree and the experimental values are 10–15 kJ/mol larger, whereas the experimental PAs for **1** and **6** are on the order of 3–5 kJ/mol higher than those predicted by theory. We have computed B3LYP/6-311++G(d,p)//B3LYP/6-31+G(d) proton affinities for all 20 ProXxx dipeptides and have obtained preliminary experimental proton affinities for 19 of the ProXxx dipeptides (Pro Arg is too basic to measure using the kinetic method) [72,73]. Figure S14 shows that twelve of the ProXxx dipeptides have preliminary experimental proton affinities that are larger than the calculated values with an average difference of +9.4 kJ/mol, whereas seven of the dipeptides have experimental proton affinities lower than the calculated value (average of −6.3). Twelve of the ProXxx dipeptides have preliminary experimental and computed proton affinities within 10 kJ/mol of each other: six above and six below. According to this chart, the extended kinetic method is overestimating the proton affinities of the dipeptides with calculated proton affinities in the range of 973–986 kJ/mol including **2**–**5** and for the three dipeptides with oxygen-atoms in the side chains. In contrast, the derived kinetic method proton affinities for the more basic dipeptides (calculated proton affinities >982 kJ/mol) are generally underestimated. We are still searching for possible causes for this behavior but at this point it is safest to consider our experimental values for **2**–**5** as upper limits.

4.4. Trends

Since a consistent set of reference bases were used for the EKM studies, we can determine a relative "effective" basicity ordering for the dipeptides in this study by examining the intensity ratios at a given collision energy. Figure S15a and b show the measured intensity ratios for **1**–**5** with piperidine (a) and the measured intensity ratios for **2**–**6** with diisopropyl amine (b) at two different lab frame collision energies (18 and 24 V). The relative ordering obtained from this data is ProGly < ProAla < ProLeu ~ ProIle ~ ProVal < ProPro, with **3**–**5** having very similar effective basicities. The similarity in effective basicity for ProVal, ProLeu, and ProIle is in accord with both the derived experimental and the isodesmic computed PA values, as is the lower basicity (PA) of ProGly and the larger basicity (PA) of ProPro. Only the anomalously high experimental PA for ProAla is in disagreement with these trends. The relative basicity ordering of ProGly and ProPro is in agreement with previous work by Cassaday using ICR bracketing [45]. The only other basicity measurement for Pro-containing dipeptides is that for ProVal from an ICR bracketing study from Gorman and Amster [42] in which they conclude that ProVal has the same gas-phase basicity as proline, which does not agree with our findings. Since the temperature was not varied in these previous studies, no direct comparisons of derived proton affinities can be made.

These relative basicities for the ProXxx dipeptides mirror those for the Xxx amino acids themselves. The proton affinities for glycine, alanine, valine, leucine, isoleucine, and proline were determined by Bouchoux and co-workers to be 887.0, 902.0, 915.0, 916.0, 919.0, and 941 kJ/mol [64]. Appending a second aliphatic amino acid to proline increases the proton affinity by 20–56 kJ depending on the residue. This increase is due to a combination of polarization effects as well as an increased stability of the cation through enhanced hydrogen bonding. The derived protonation entropies range from −20 to −40 J mol^{-1} K^{-1} and are consistent with the increase in hydrogen bonding in the cations relative to the neutrals. The lowest energy conformers for **1**–**5** all have a hydrogen bond between the ring nitrogen and the amide N-H of ~2.15 Å. Upon protonation, the ring nitrogen is no longer able to be an H-bond acceptor and thus the preferred H-bond scheme in **1H – 5H** switches to one in which the ring nitrogen is a H-bond donor to the amide carbonyl oxygen. The average H-bond distance decreases to ~1.8 Å. The "syn" arrangement of the amide carbonyl oxygen with respect to the ring nitrogen atom puts the amide NH group in the "anti" position allowing for an additional H-bond with the C-terminal carbonyl oxygen atom. For ProPro, the lack of an amide NH group in the neutral results in similar H-bonding arrangements in both the neutral and the cation. In the neutral, the N-O distance is ~2.17 Å, which drops to ~1.78 Å in the cation. This still represents a decrease in entropy upon protonation, but the similarity between the geometries of **6** and **6H** result in a smaller negative protonation entropy than those for **2**–**5** and an isothermal crossing point that is closer to the apparent gas-phase basicity.

The computed proton affinities for ProXxx track the proton affinities of Xxx as shown in Figure S16, which makes sense as the proline residue remains constant and the second residue contributes mainly to the overall polarizability of the molecule. Figure S16 also shows that calculated proton affinities for the amide nitrogen atom (Table S3) also track the proton affinities of the amino group in Xxx. Finally, the calculated amide oxygen atom proton affinities (Table S3) track the amino group proton affinities of Xxx for **1**–**5**, but the amide oxygen proton affinity of **6** is much lower than would be predicted by the simple trends. ProPro was one of the residue combinations that was found to be resistant to cleavage [26,29] and this could be a result of the decreased PA of the amide group during proton transfer after collisional activation. Further insight into the relationship between amide oxygen proton affinity and fragmentation efficiency will be discussed in a future publication on XxxPro proton affinities [74].

5. Conclusions

We have measured the proton affinities of six proline-containing dipeptides using the extended kinetic method in an electrospray ionization – triple quadrupole instrument. The ProXxx dipeptides are significantly (20–50 kJ/mol) more basic than proline itself due to the larger polarizabilities of the dipeptides and the increased hydrogen bonding in the cations. The proton affinities of ProXxx generally track the proton affinities of the Xxx amino acids. Unlike in our previous studies on amino acid thermochemistry in which we saw excellent agreement between kinetic method derived proton affinities and those derived from density functional calculations, the agreement for the proton affinities for the dipeptides in this study is less satisfying. For ProGly and ProPro, the experimental proton affinities are within 3–6 kJ/mol, well within the experimental uncertainties. However, for ProVal, ProLeu, and ProIle, the calculated proton affinities are *ca.* 10 kJ/mol lower than the experimental values and for ProAla, the difference is 14.5 kJ/mol. Multiple different single-point energy calculations at B3LYP/6-31+G(d,) geometries give proton affinity predictions that are within 5 kJ/mol of each other for all dipeptides. In addition, re-optimization at M06-2x shows only minor differences in the relative energy ordering of the low-energy conformers and the Boltzmann-weighted proton affinities are within 5 kJ/mol of the B3LYP results. The kinetic method is likely giving anomalously high proton affinities, due in part to the large entropy in these systems which requires extrapolation to the isothermal point in the workup. This is further shown by examining the relative "effective gas-phase basicities" obtained from single reference bases without extrapolation. Further investigations into the cause of this behavior are ongoing, so we recommend the experimental proton affinities for ProGly and ProPro and the calculated values for the proton affinities of **2**–**5** with the experimental values as upper limits.

CRediT authorship contribution statement

Henry Cardwell: Investigation, Formal analysis, Data curation. **Paul Acoria:** Investigation, Formal analysis. **Alexis Brender A Brandis:** Investigation, Formal analysis, Data curation. **Kathy Huynh:** Investigation, Formal analysis, Data curation. **Madeleine Lamb:** Formal analysis, Data curation. **Sophie Messinger:** Investigation, Formal analysis. **Daria Moody:** Investigation, Data curation. **Laurel Nicks:** Formal analysis, Data curation. **Hao Qian:** Investigation, Data curation. **Marcus Quint:** Investigation, Formal analysis, Data curation. **Trinh Ton:** Investigation, Formal analysis, Data curation. **Anna Grace Towler:** Investigation, Formal analysis, Data curation. **Michael Valasquez:** Investigation, Formal analysis, Data curation. **Jennifer Poutsma:** Validation, Supervision, Project administration, Methodology, Investigation, Funding acquisition, Formal analysis, Data curation, Conceptualization. **John C. Poutsma:** Writing – review & editing, Writing – original draft, Validation, Supervision, Resources, Project administration, Methodology, Investigation, Funding acquisition, Formal analysis, Data curation, Conceptualization.

Declaration of competing interest

The authors declare that they have no known competing financial interests or personal relationships that could have appeared to influence the work reported in this paper.

Acknowledgements

Funding for this project was generously provided by the National Science Foundation (CHE1464763, CHE1800137, CHE2154537). Henry Cardwell acknowledges the Beckman Foundation for a Beckman Scholar Award.

Appendix A. Supplementary data

Supplementary data to this article can be found online at https://doi.org/10.1016/j.ijms.2024.117352.

Data availability

Data will be made available on request.

References

[1] T.E. Angel, U.K. Aryal, S.M. Hengel, E.S. Baker, R.T. Kelly, E.W. Robinson, R. D. Smith, Mass spectrometry-based proteomics: existing capabilities and future directions, Chem. Soc. Rev. 41 (2012) 3912.
[2] P. Roepstorff, Mass spectrometry based proteomics, background, status, and future needs, Protein Cell 3 (2012) 641.
[3] E. Sabido, N. Selevsek, R. Aebersold, Mass spectrometry-based proteomics for systems biology, Curr. Opin. Biotechnol. 23 (2012) 591.
[4] Kelleher, Status of mass spectrometry-based proteomics and metabolomics in basic and translational research, Biochemist 52 (2013) 3794.
[5] Y. Zahang, B.R. Fonslow, B. Shan, M.-C. Baek, J.R. Yates, Protein analysis by shotgun/bottom-up proteomics, Chem. Rev. 113 (2013) 2343.
[6] P. Roepstorff, Proposal for a common nomenclature for sequence ions in mass spectra of peptides, Biomed. Mass Spectrom. 11 (1984) 601.
[7] B. Paizs, S. Suhai, Fragmentation pathways of protonated peptides, Mass Spectrom. Rev. 24 (2005) 508.

[8] K.A. Cox, S.J. Gaskell, M. Morris, A. Whiting, Role of the site of protonation in the low-energy decompositions of gas-phase peptide ions, J. Am. Soc. Mass Spectrom. 7 (1996) 522.

[9] A.R. Dongre, J.L. Jones, A. Somagyi, V.H. Wysocki, Influence of peptide composition, gas-phase basicity, and chemical modification on fragmentation efficiency: evidence for the mobile proton model, J. Am. Chem. Soc. 118 (1996) 8365.

[10] V.H. Wysocki, G. Tsaprailis, L.L. Smith, L.A. Breci, Mobile and localized protons: a framework for understanding peptide dissociation, J. Mass Spectrom. 35 (2000) 1399.

[11] J.K. Eng, A.L. McCarmack, J.R. Yates III, An approach to correlate tandem mass spectral data of peptides with amino acid sequences in a protein database, J. Am. Soc. Mass Spectrom. 5 (1994) 976.

[12] D.N. Perkins, D.J.C. Pappin, D.M. Creasy, J.S. Cottrell, Probability-based protein identification by searching sequence databases using mass spectrometry data, Electrophoresis 20 (1999) 3551.

[13] R. Craig, R.C. Beavis, TANDEM: matching proteins with tandem mass spectra, Bioinformatics 20 (2004) 1466.

[14] J.E. Elias, F.D. Gibbons, O.D. King, F.P. Roth, S.P. Gygi, Intensity-based protein identification by machine learning from a library of tandem mass spectra, Nat. Biotechnol. 22 (2004) 214.

[15] W. Li, L. Ji, J. Goya, G. Tan, V.H. Wysocki, SQID: an intensity-incorporated protein identification algorithm for tandem mass spectrometr, J. Proteome Res. 10 (2011) 1593.

[16] B.L. Schwartz, M.M. Bursey, Some proline substituent effects in the tandem mass spectrum of protonated pentaalanine, Biol. Mass Spectrom. 21 (1992) 92.

[17] J.A. Loo, C.A. Edmonds, R.D. Smith, Tandem mass spectrometry of very large molecules. 2. Dissociation of multiply charged proline-containing proteins from electrospray ionization, Anal. Chem. 65 (1993) 425.

[18] W. Yu, J.E. Vath, M.C. Huberty, S.A. Martin, Identification of the facile gas-phase cleavage of the Asp-pro and Asp-Xxx peptide bonds in matrix-assisted laser desorption time of flight mass spectrometry, Anal. Chem. 65 (1993) 3015.

[19] T. Vaisar, J. Urban, Probing the proline effect in CID of protonated peptides, J. Mass Spectrom. 31 (1996) 1185.

[20] T.G. Schaaff, B.J. Cargile, M.S. Stephanson, Ion trap activation of the $(M+2H)2^{+}$ and $(M+17H)1^{7+}$ ions of human hemoglobin β-chain, Anal. Chem. 72 (2000) 899.

[21] G. Tsaprailis, A. Somogyi, E.N. Nikolaev, V.H. Wysocki, Refining the model for selective cleavage at acid residues in arginine-containing protonated peptides, Int. J. Mass Spectrom. 195/196 (2000) 467.

[22] A.G. Sullivan, F.L. Brancia, R. Tyldesley, R. Bateman, K. Sidhu, S.J. Hubbard, S. G. Oliver, S.J. Gaskell, The exploitation of selective cleavage of singly protonated peptide ions adjacent to aspartic acid residues using a quadrupole orthogonal time-of-flight mass spectrometer equipped with a matrix-assisted laser desorption/ ionization source, Int. J. Mass Spectrom. 2011 (2001) 665.

[23] Y. Huang, V.H. Wysocki, D.L. Tabb, J.R.I. Yates, The influence of histidine on cleavage C-terminal to acidic residues in doubly protonated tryptic peptides, Int. J. Mass Spectrom. 291 (2002) 233.

[24] L.A. Breci, D.L. Tabb, J.R.I. Yates, V.H. Wysocki, Cleavage N-terminal to proline: analsis of a database of peptide tandem mass spectra, Anal. Chem. 75 (2003) 1963.

[25] R.N. Grewal, E.H. El Aribi, A.G. Harrison, K.W.M. Siu, A.C. Hopkinson, Fragmentation of protonated tripeptides: the proline effect revisited, J. Phys. Chem. B 108 (2004) 4899.

[26] Y. Huang, J.M. Triscari, G.C. Tseng, L. Pasa-Tolic, M.S. Lipton, R.D. Smith, V. H. Wysocki, Statistical characterization of the charge state and residue dependence of low-energy CID peptide dissociation patterns, Anal. Chem. 77 (2005) 5800.

[27] A.G. Harrison, A.B. Young, Fragmentation reactions of deprotonated peptides containing proline. The proline effect, J. Mass Spectrom. 40 (2005) 1173.

[28] A.G. Unnithan, M.J. Myer, C.J. Veale, A.S. Dannell, MS/MS of protonated polyproline peptides; the influence of N-terminal protonation on dissociation, J. Am. Soc. Mass Spectrom. 18 (2007) 2198.

[29] Y. Huang, G.C. Tseng, S. Yuan, L. Pasa-Tolic, M.S. Lipton, R.D. Smith, V. H. Wysocki, A data mining scheme for identifying peptide structural motifs responsible for different MS/MS fragmentation intensity patterns, J. Proteome Res. 7 (2008) 70.

[30] C. Bleiholder, S. Suhai, A.G. Harrison, B. Paizs, Towards understanding the tandem mass spectra of protonated oligopeptides. 2: the proline effect in collision-induced dissociation of protonated Ala-Ala-Xxx-Pro-Ala (Xxx = Ala, ser, Leu, val, Phe, and Trp), J. Am. Soc. Mass Spectrom. 21 (2011) 1032.

[31] Q. Zhang, B. Perkins, G. Tan, V.H. Wysocki, The role of proton bridges in selective cleavage of Ser-, Thr-, Cys-, Met-, Asp-, and Asn-containing peptides, Int. J. Mass Spectrom. 300 (2011) 108.

[32] W.M. McGee, S.A. McLuckey, The ornithine effect in peptide cation dissociation, J. Mass Spectrom. 48 (2013) 856.

[33] A.F. Kuntz, A.W. Boynton, G.A. David, K.E. Colyer, J.C. Poutsma, Proton affinities of proline analogs using the kinetic method with full entropy analysis, J. Am. Soc. Mass Spectrom. 13 (2002) 72.

[34] S. Gronert, D.C. Simpson, K.M. Conner, A reevaluation of computed proton affinities for the common α-amino acids, J. Am. Soc. Mass Spectrom. 20 (2009) 2116.

[35] G. Bouchoux, S. Huang, B.S. Inda, Acid-base thermochemistry of gaseous aliphatic α-amino acids, Phys. Chem. Chem. Phys. 13 (2011) 651.

[36] M.M. Raulfs, L. Breci, M. Bernier, O. Hamdy, A. Janiga, V.H. Wysocki, J. C. Poutsma, Investigations of the mechanism of the "proline effect" in mass spectrometry peptide fragmentation experiments: the "pipecolic acid effect, J. Am. Soc. Mass Spectrom. 25 (2014) 1705.

[37] M.T. Abutokaikah, S. Guan, B.J. Bythell, Stereochemical sequence ion selectivity: proline versus pipecolic- acid- containing protonated peptides, J. Am. Soc. Mass Spectrom. 28 (2017) 182.

[38] A.F. DeBlase, C.P. Harrilal, J.T. Lawler, N.L. Burke, S.A. McLuckey, T.S. Zwier, Conformation- specific infrared and ultraviolet spectroscopy of cold [YAPAA+H] + and [YGPAA+H] + ions: a stereochemical "twist" on the β- Hairpin turn, J. Am. Chem. Soc. 139 (2017) 5481.

[39] A.C. Gucinski, J. Chamot-Rooke, V. Steinmetz, A. Somogyi, V.H. Wysocki, Influence of N-terminal residue composition on the structure of proline-containing $b2_{+}$ ions, J. Phys. Chem. A 117 (2013) 1291.

[40] J.K. Martens, J. Grzetic, G. Berden, J. Oomens, Gas- phase conformations of small polyprolines and their fragment ions by IRMPD spectroscopy, Int. J. Mass Spectrom. 377 (2015) 179.

[41] J.C. Poutsma, J.K. Martens, J. Oomens, P. Maitre, V. Steinmetz, M. Bernier, M. Jia, V.H. Wysocki, Infrared multiple- photon dissociation action spectroscopy of the $b2_{+}$ ion from PPG: evidence of third residue affecting $b2_{+}$ fragment structure, J. Am. Soc. Mass Spectrom. 28 (2017) 1482.

[42] G.S. Gorman, I.J. Amster, Gas phase basicity measurements of dipeptides that contain valine, J. Am. Chem. Soc. 115 (1993) 5729.

[43] C.J. Cassaday, S. Carr, K. Zhang, A. Chung-Phillips, Experimental and ab initio studies on protonations of alanine and small peptides of alanine and Glycine, J. Org. Chem. 60 (1995) 1704.

[44] S.R. Carr, C.J. Cassady, Gas-phase basicities of histidine and lysine and their selected di- and tripeptides, J. Am. Chem. Soc. Mass Spectrom 7 (1996) 1203.

[45] N.P. Ewing, X. Zhang, C.J. Cassady, Determination of the gas-phase basicities of proline and its di- and tripeptides with Glycine: the enhanced basicity of prolylproline, J. Mass Spectrom. 31 (1996) 1345.

[46] J.W. McKiernan, C.E. Beltrame, C.J. Cassady, Gas-phase basicities of serine and dipeptides of serine and Glycine, J. Am. Soc. Mass Spectrom. 5 (1994) 718.

[47] J. Perez, L.E. Ramirez-Arizmendi, C.J. Petzold, L.P. Guler, E.D. Nelson, H. I. Kenttamaa, Laser-induced acoustic desorption/chemical ionization in fourier-transform ion cyclotron resonance mass spectrometry, Int. J. Mass Spectrom. 198 (2000) 173.

[48] I. Webb, C. Muetterties, C.B. Platner, J.C. Poutsma, Gas-phase acidities of lysine homologues and proline analogs from the extended kinetic method, Int. J. Mass Spectrom. 316–318 (2012) 126.

[49] R.G. Cooks, J.S. Patrick, T. Kotiaho, S.A. McLuckey, Thermochemical determinations by the kinetic method, Mass Spectrom. Rev. 18 (1994) 287.

[50] Z. Wu, C. Fenselau, Gas-phase basicities and proton affinities of lysine and histidine measured from the dissociation of proton-bound dimers, Rapid Commun. Mass Spectrom. 8 (1994) 777.

[51] B.A. Cerda, C. Wesdemiotis, Li+, Na+' and K+ binding to the DNA and RNA nucleobases. Bond energies and attachment sites from the dissociation of metal ion-bound heterodimers, J. Am. Chem. Soc. 118 (1996) 11884.

[52] P.B. Armentrout, Entropy measurements and the kinetic method: a statistically meaningful approach, J. Am. Soc. Mass Spectrom. 11 (2000) 371.

[53] K.M. Ervin, P.B. Armentrout, Systematic and random errors in ion affinities and activation entropies from the extended kinetic method, J. Mass Spectrom. 39 (2004) 1004.

[54] M.J. Frisch, G.W. Trucks, H.B. Schlegel, G.E. Scuseria, M.A. Robb, J.R. Cheeseman, G. Scalmani, V. Barone, B. Mennucci, G.A. Petersson, H. Nakatsuji, M. Caricato, X. Li, H.P. Hratchian, A.F. Izmaylov, J. Bloino, G. Zheng, J.L. Sonnenberg, M. Hada, M. Ehara, K. Toyota, R. Fukuda, J. Hasegawa, M. Ishida, T. Nakajima, Y. Honda, O. Kitao, H. Nakai, T. Vreven, J.A. Montgomery Jr., J.E. Peralta, F. Ogliaro, M. Bearpark, J.J. Heyd, E. Brothers, K.N. Kudin, V.N. Staroverov, R. Kobayashi, J. Normand, K. Raghavachari, A. Rendell, J.C. Burant, S.S. Iyengar, J. Tomasi, M. Cossi, N. Rega, J.M. Millam, M. Klene, J.E. Knox, J.B. Cross, V. Bakken, C. Adamo, J. Jaramillo, R. Gomperts, R.E. Stratmann, O. Yazyev, A.J. Austin, R. Cammi, C. Pomelli, J.W. Ochterski, R.L. Martin, K. Morokuma, V.G. Zakrzewski, G.A. Voth, P. Salvador, J.J. Dannenberg, S. Dapprich, A.D. Daniels, Ö. Farkas, J. B. Foresman, J.V. Ortiz, J. Cioslowski, D.J. Fox, Gaussian 09, Revision E.01 E. 01, Gaussian, Inc., Wallingford, CT, 2013.

[55] M.J. Frisch, G.W. Trucks, H.B. Schlegel, G.E. Scuseria, M.A. Robb, J.R. Cheeseman, G. Scalmani, V. Barone, G.A. Petersson, H. Nakatsuji, X. Li, M. Caricato, A. V. Marenich, J. Bloino, B.G. Janesko, R. Gomperts, B. Mennucci, H.P. Hratchian, J. V. Ortiz, A.F. Izmaylov, J.L. Sonnenberg, F. Williams Ding, F. Lipparini, F. Egidi, J. Goings, B. Peng, A. Petrone, T. Henderson, D. Ranasinghe, V.G. Zakrzewski, J. Gao, N. Rega, G. Zheng, W. Liang, M. Hada, M. Ehara, K. Toyota, R. Fukuda, J. Hasegawa, M. Ishida, T. Nakajima, Y. Honda, O. Kitao, H. Nakai, T. Vreven, K. Throssell, J.A. Montgomery, J.E. Peralta, F. Ogliaro, M.J. Bearpark, J.J. Heyd, E. N. Brothers, K.N. Kudin, V.N. Staroverov, T.A. Keith, R. Kobayashi, J. Normand, K. Raghavachari, A.P. Rendell, J.C. Burant, S.S. Iyengar, J. Tomasi, M. Cossi, J. M. Millam, M. Klene, C. Adamo, R. Cammi, J.W. Ochterski, R.L. Martin, K. Morokuma, O. Farkas, J.B. Foresman, D.J. Fox, Gaussian 16 Rev. C.01 Wallingford, CT, 2016.

[56] PCModel Serena Software, 2006.

[57] C. Lee, W. Yang, R.G. Parr, Development of the colle-salvetti correlation energy formula into a functional of the electron density, Phys. Rev. B 37 (1988) 785.

[58] A.D. Becke, Density functional thermochemistry. III. The role of exact exchange, J. Chem. Phys. 98 (1993) 5648.

[59] O.E. Schroeder, E.J. Andriole, K.L. Carver, J.C. Poutsma, The proton affinity of lysine analogs using the extended kinetic method, J. Phys. Chem. A 108 (2004) 326.

[60] E.J. Andriole, K.E. Colyer, E. Cornell, J.C. Poutsma, Proton affinity of canavanine and canaline, oxy-analogs of arginine and ornithine, from the extended kinetic method, J. Phys. Chem. A 110 (2006) 11501.

[61] C. Muetterties, A. Drissi Touzani, I. Hardee, K.T. Huynh, J.C. Poutsma, Gas-phase acid-base properties of 1-aminocycloalkane-1-carboxylic acids from the extended kinetic method, Int. J. Mass Spectrom. 378 (2015) 59.
[62] C. Muetterties, A. Janiga, K.T. Huynh, M.G. Pisano, V.T. Tripp, D.D. Young, J. C. Poutsma, Gas-phase acid-base properties of homocysteine, homoserine, 5-mercaptonorvaline, and 5-hydroxynorvaline from the extended kinetic method, Int. J. Mass Spectrom. 369 (2014) 71.
[63] G.A. Turner, D. Long, E. Owens, E.S. Iqbal, M.C.T. Hartman, J.C. Poutsma, Acid/base properties of α-methyl and gem-dimethyl derivatives of cysteine and serine from the extended kinetic method, Int. J. Mass Spectrom. 475 (2022) 116833.
[64] E.P. Hunter, S.G. Lias, Evaluated gas-phase basicities and proton affinities of molecules: an update, J. Phys. Chem. Ref. Data 27 (1998) 3.
[65] S. Grimme, J. Antony, S. Ehrlich, H. Krieg, A consistent and accurate ab initio parameterization of density functional dispersion correction (DFT-D) for the 94 elements H-Pu, J. Chem. Phys. 132 (2010) 154104.
[66] M.J. Frisch, M. Head-Gordon, J.A. Pople, Direct MO2 gradient method, Chem. Phys. Lett. 166 (1990) 275.
[67] Y. Zhao, D.G. Truhlar, The M06 suite of density functionals for main group thermochemistry, thermochemical kinetics, noncovalent interactions, excited states, and transition elements: two new functionals and systematic testing of four M06-class functionals and 12 other functionals, Theor. Chem. Acc. 120 (2008) 215.
[68] G. Bouchoux, F. Djazi, F. Gaillard, D. Vierezet, Application of the kinetic method to bifunctional bases. MIKE and CID-MIKE test cases, Int. J. Mass Spectrom. 227 (2003) 479.
[69] G. Bouchoux, D.-A. Buisson, S. Bourcier, M. Sablier, Application of the kinetic method to bifunctional bases. ESI tandem quadrupole experiments, Int. J. Mass Spectrom. 228 (2003) 1035.
[70] J.C. Cao, C. Aubry, J.L. Holmes, Proton affinities of simple amine: entropies and enthalpies of activation and their effect on the kinetic method for evaluating proton affinities, J. Phys. Chem. A 104 (2000) 10045.
[71] I.S. Hahn, C. Wesdemiotis, Protonation thermochemistry of β-alanine. An evaluation of the proton affinities and entropies determined by the extended kinetic method, Int. J. Mass Spectrom. 222 (2003) 465.
[72] Cardwell, H.; Arcoria, P.; Brender A Brandis, A.; Farmer, S.; Glass, S.; Messinger, S.; Moody, D.; Nicks, L.; Qian, H.; Quint, M.; Ton, T.; Towler, A. G.; Turner, G. A.; Vallejo, R.; Velasquez, M.; Poutsma, J. L.; Poutsma, J. C. "Gas-phase Proton Affinities of Proline Containing Dipeptides. 2 ProCys, ProMet, ProSer, ProThr, ProTyr, ProPhe, and ProTrp."to be published.
[73] Cardwell, H.; Arcoria, P.; Brender A Brandis, A.; Farmer, S.; Glass, S.; Messinger, S.; Moody, D.; Nicks, L.; Qian, H.; Quint, M.; Ton, T.; Towler, A. G.; Turner, G. A.; Vallejo, R.; Velasquez, M.; Poutsma, J. L.; Poutsma, J. C. Gas-phase proton affinities of proline containing dipeptides. 3: ProArg, ProLys, ProHis, ProAsp, ProAsn, ProGlu, ProGln."to be published.
[74] Ton, T.; Arcoria, P.; Cardwell, H.; Farmer, S.; Glass, S.; Huynh, K. T.; Messinger, S.; Moody, D.; Qian, H.; Quint, M.; Towler, A. G.; Velasquez, M.; Poutsma, J. L.; Poutsma, J. C. "Gas-phase Proton Affinities of Proline Containing Dipeptides. 4. Proton Affinities for XxxPro Dipeptides.", to be published.